

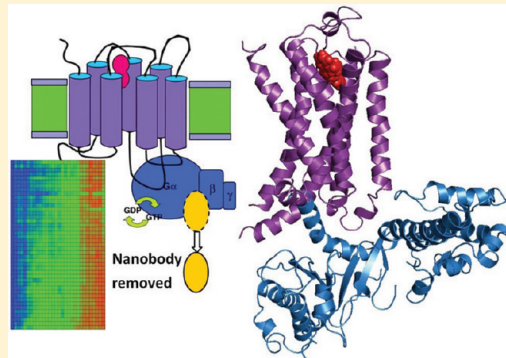
# Studies on the Interactions between $\beta_2$ Adrenergic Receptor and Gs Protein by Molecular Dynamics Simulations

Zhiwei Feng, Tingjun Hou, and Youyong Li\*

Institute of Functional Nano & Soft Materials (FUNSOM) and Jiangsu Key Laboratory for Carbon-Based Functional Materials & Devices, Soochow University, Suzhou, Jiangsu 215123, China

## Supporting Information

**ABSTRACT:** The  $\beta_2$  adrenergic receptor ( $\beta_2$ AR) plays a key role in the control of smooth muscle relaxation in airways, the therapy of asthma, and a series of other basic physiological functions. Recently, the crystal structure of the  $\beta_2$ AR–Gs protein complex was reported, which facilitates study of the activation mechanism of the  $\beta_2$ AR and G-protein-coupled receptors (GPCRs). In this work, we perform 20 ns molecular dynamics (MD) simulations of the  $\beta_2$ AR–Gs protein complex with its agonist in an explicit lipid and water environment to investigate the activation mechanism of  $\beta_2$ AR. We find that during 20 ns MD simulation with a nanobody bound the interaction between the  $\beta_2$ AR and the Gs protein is stable and the whole system is equilibrated within 6 ns. However, without a nanobody stabilizing the complex, the agonist triggers conformational changes of  $\beta_2$ AR sequentially from the extracellular region to the intracellular region, especially the intracellular parts of TM3, TMS, TM6, and TM7, which directly interact with the Gs protein. Our results show that the  $\beta_2$ AR–Gs protein complex makes conformational changes in the following sequence: (1) an agonist-bound part of  $\beta_2$ AR, (2) the intracellular region of  $\beta_2$ AR, and (3) the Gs protein.



## 1. INTRODUCTION

$\beta_2$ AR<sup>1–7</sup> is a member of the  $\beta$  adrenergic receptor ( $\beta$ AR)<sup>8–12</sup> family. The adrenergic receptor family consists of  $\beta_1$  adrenergic receptor ( $\beta_1$ AR),<sup>13,14</sup>  $\beta_2$  adrenergic receptor ( $\beta_2$ AR), and  $\beta_3$  adrenergic receptor ( $\beta_3$ AR),<sup>15–17</sup> and it plays a key role in regulating cardiac function,<sup>18</sup> which belongs to class A of G-protein-coupled receptors (GPCRs).<sup>19–24</sup>

$\beta_2$ AR is widely expressed in the pulmonary and cardiac myocyte tissue<sup>25</sup> and activated by adrenaline that plays an important part in cardiovascular and pulmonary physiology.  $\beta_2$ AR plays a key role in the control of smooth muscle relaxation in airways,<sup>26,27</sup> the therapy of asthma,<sup>28–31</sup> the stimulation of the heart,<sup>32,33</sup> and a series of other basic physiological functions.<sup>34</sup>

$\beta_2$ AR is an ideal model system<sup>1–7</sup> not only because it is important in medicinal chemistry, for example,  $\beta_2$ AR expressed on the airway smooth muscle are targets for  $\beta$  agonists used in treatment of asthma, and so an active state model would greatly facilitate structure-based agonist design. Also, because  $\beta_2$ AR is widely used in signal transduction studies, there is a wealth of experimental data to validate the active state models.

In 2007, Rasmussen and co-workers reported the crystal structure of  $\beta_2$ AR.<sup>3</sup> It differed from rhodopsin,<sup>35</sup> and there were weak interactions between the cytoplasm ends of transmembrane TM3 and TM6 involving the conserved Glu/Asp-Arg-Tyr(E/DRY) sequence, which might be responsible for the relatively high basal activity and structural instability of  $\beta_2$ AR and contributed to the challenges in obtaining diffraction-

quality crystals of nonrhodopsin GPCRs. In 2011, Rasmussen et al.<sup>7</sup> reported the crystal structure of a nanobody-stabilized active state of  $\beta_2$ AR. They used a camelid antibody fragment (the nanobody (Nb35) was the recombinant minimal-sized intact antigen-binding domain of such a camelid heavy chain antibody and was approximately 25% the size of a conventional Fab fragment) to stabilize the human  $\beta_2$ AR and obtained an agonist-bound, active-state crystal structure of the receptor–nanobody complex. Compared with the inactive  $\beta_2$ AR structure, it revealed subtle changes in the binding pocket. These changes were associated with an 11 Å outward movement of the cytoplasmic end of TM6 and rearrangements of TMS and TM7 that were remarkably similar to those observed in opsin, an active form of rhodopsin.

Recently, the crystal structure of the  $\beta_2$ AR–Gs protein complex was reported by Rasmussen et al.,<sup>2</sup> and it consisted of an agonist-occupied active state monomeric  $\beta_2$ AR and a nucleotide-free Gs heterotrimer. The principal interactions between  $\beta_2$ AR and Gs involved the amino- and carboxy-terminal  $\alpha$ -helix of Gs. Compared with the inactive structure of  $\beta_2$ AR, the largest conformational change in the active  $\beta_2$ AR was a 14 Å outward movement at the cytoplasmic end of TM6 and an  $\alpha$ -helix extension of the cytoplasmic end of TMS. This was the first structure that provided the structural details of the interaction between GPCR and the Gs protein.

**Received:** December 12, 2011

**Published:** March 10, 2012



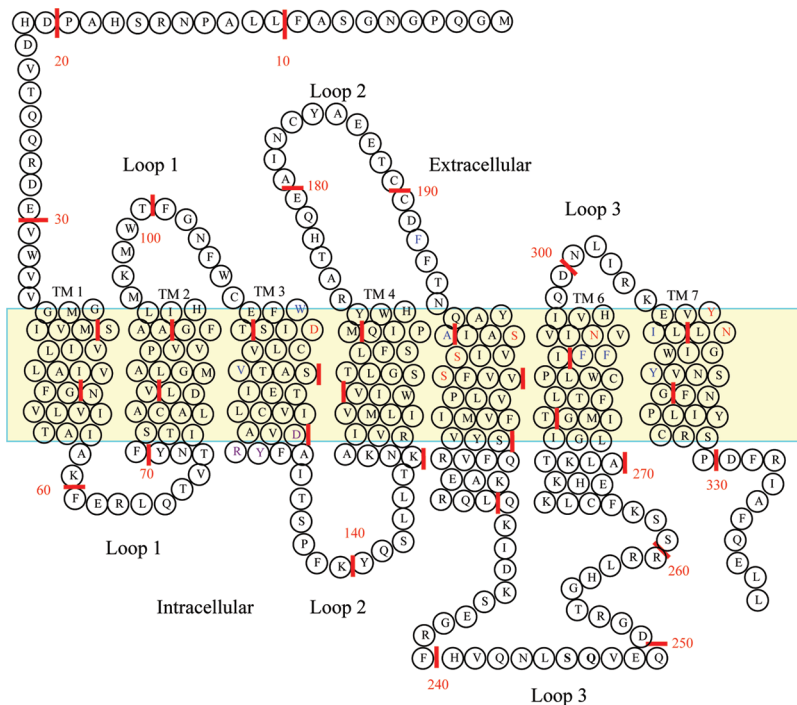


**Figure 1.** Schematic diagram of the sequence of  $\beta_2$ AR. Amino acids highlighted in red have been shown to be important for agonist binding by mutation (D113<sup>3,32</sup>, S203<sup>5,42</sup>, S204<sup>5,43</sup>, S207<sup>5,48</sup>, N293<sup>6,55</sup>, N308<sup>7,35</sup>, S312<sup>7,39</sup>). Residues highlighted in blue show hydrophobic interactions with the agonist BI-167107 (W109<sup>3,28</sup>, V117<sup>3,36</sup>, F193<sup>5,32</sup>, A200<sup>5,39</sup>, F289<sup>6,51</sup>, F290<sup>6,52</sup>, I309<sup>7,36</sup>, Y316<sup>7,43</sup>).

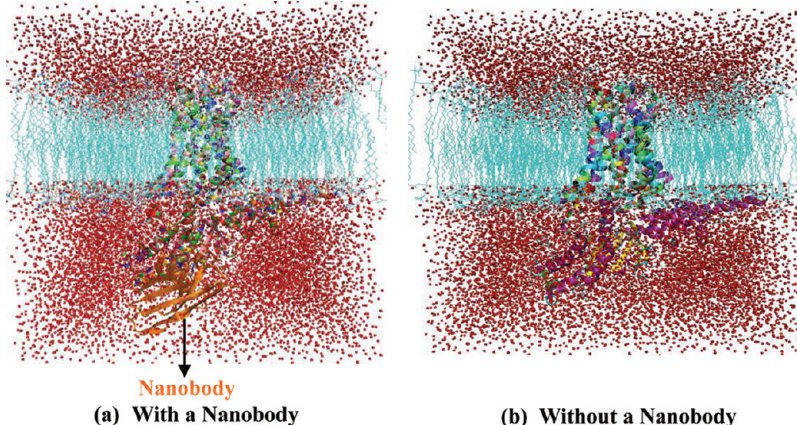


**Figure 2.** MD simulation box of the  $\beta_2$ AR–Gs protein complex with lipid and water (without a nanobody, T4L, G $\beta$ , and G $\gamma$ ). EC (extracellular) region is at the top. There are  $\sim$ 101 500 atoms in the simulation box.

This crystal structure only represents a static state, and the dynamic processes and the underlying mechanisms remain unknown. The nanobody in this crystal structure<sup>2</sup> is used to stabilize the active state of  $\beta_2$ AR to prepare the crystal. We first perform 20 ns MD simulation with a nanobody bound and find that the interaction between the  $\beta_2$ AR and the Gs protein is stable and the whole system is equilibrated within 6 ns. Then we remove the nanobody from the crystal structure<sup>2</sup> and perform molecular dynamics (MD) simulations to study the dynamic processes and the underlying mechanisms of interactions between an agonist-bound  $\beta_2$ AR and Gs protein. Our results show sequential conformational changes in the  $\beta_2$ AR–Gs protein complex, which provide a structural basis for the activation mechanism of  $\beta_2$ AR and other GPCRs.

## 2. MATERIALS AND METHODS

**2.1. Protein Structures.** The crystal structure of the  $\beta_2$  adrenergic receptor ( $\beta_2$ AR)–Gs protein complex<sup>2</sup> (PDB entry 3SN6, resolution 3.20 Å) is used. The  $\beta_2$ AR, agonist BI-167107 (BI-167107, Boehringer Ingelheim), G $\alpha_{\text{Ras}}$  (the Ras-like GTPase domain), and G $\alpha_{\text{AH}}$  (the  $\alpha$ -helical domain) in the crystal structure are separated from the  $\beta_2$ AR–Gs protein complex and used for MD simulations. The nanobody is used to stabilize an active state of  $\beta_2$ AR to prepare the crystal structure. In order to study the interaction between the agonist-bound  $\beta_2$ AR and Gs protein we retain/remove the nanobody from the crystal structure to perform parallel molecular dynamics simulations. We do not include the T4L (T4 lysozyme), G $\beta$ , and G $\gamma$  (the Gs heterotrimer includes three subunits:  $\alpha$ ,  $\beta$ , and  $\gamma$ ; the GTP binds to the nucleotide-free  $\alpha$  subunit resulting in dissociation of the  $\alpha$  and  $\beta\gamma$  subunits from

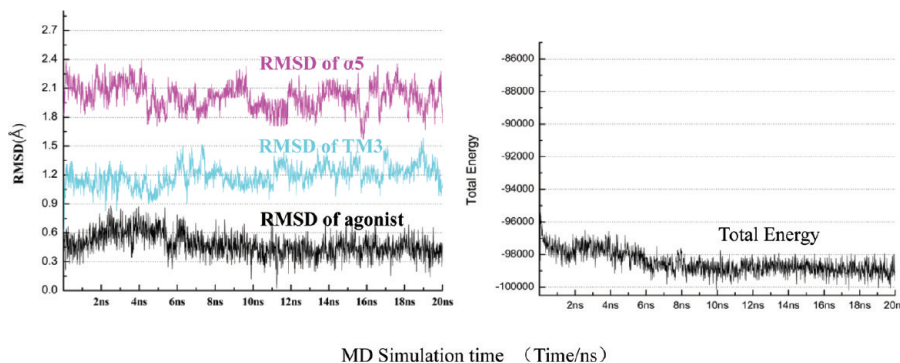


**Figure 3.** With a nanobody bound, the interaction between the  $\beta_2$ AR and the G protein is stable and the whole system is equilibrated within 6 ns.

the receptor) in MD simulations, since they are not directly involved in the interaction between the  $\beta_2$ AR and the Gs protein, which may show insignificant interaction indirectly. Figure 1 shows a schematic diagram of the sequence of  $\beta_2$ AR. Amino acids highlighted in red have been shown to be important for agonist binding by mutation. Residues highlighted in blue show the hydrophobic interactions with the agonist BI-167107.

**2.2. Molecular Dynamics Simulations.** The crystal structure of the  $\beta_2$  adrenergic receptor ( $\beta_2$ AR)-Gs protein complex<sup>2</sup> is obtained from the Protein Data Bank (PDB entry 3SN6, resolution 3.20 Å). The missing residues at the N- and C-terminals (also at loops) are not considered. The molecular topology file for the agonist BI-167107 is generated by VEGA ZZ.<sup>36</sup> Then the complex is embedded in a periodic structure of 1-palmytoyl-2-oleoyl-sn-glycero-3-phosphatidylcholine (POPC) using the VMD<sup>37</sup> program. The lipid molecules within 5 Å of the complex are eliminated. Then we insert it into a water box (TIP3<sup>38</sup> water model) and eliminate the waters within 5 Å of the lipid and protein. The whole system is built up using the VMD<sup>37</sup> program.

The whole system (Figure 2) includes the  $\beta_2$ AR, agonist BI-167107,  $G\alpha_{Ras}$ ,  $G\alpha_{AH}$ , 265 lipid molecules, ~18 619 water molecules, and 1 sodium ion for a total of ~101 500 atoms per periodic cell. The box size is 110 Å × 110 Å × 110 Å. The system is first equilibrated for 500 ps with the protein fixed under constant temperature (310 K) and constant pressure (1 atm) conditions. Then the protein is released and another 1 ns equilibration is performed.

Our MD simulations were performed using the NAMD<sup>39</sup> package (version 2.7b2) with the CHARMM<sup>40–42</sup> force field for the studied complex with explicit water and periodically infinite lipid. Electrostatics are calculated using the particle mesh Ewald (PME)<sup>43</sup> method with a 12 Å nonbonded cutoff. Temperature and pressure are kept constant using a langevin thermostat and langevin barostat, respectively. The time step of MD simulations is set to 1 fs. Data are saved every 10 ps for analysis. Twenty nanosecond MD simulation is performed under a constant temperature of 310 K and a constant pressure of 1 atm. Trajectory analyses are carried out with VEGA ZZ and VMD.<sup>36,37</sup>

### 3. RESULTS AND DISCUSSION

**3.1. Twenty Nanosecond Molecular Dynamics Simulation with a Nanobody.** We first perform 20 ns MD simulation with a nanobody bound, which is used to stabilize the complex by Rasmussen.<sup>2</sup> We find that during 20 ns MD simulation with a nanobody bound the interaction between the

$\beta_2$ AR and the Gs protein is stable and the whole system is equilibrated within 6 ns. Figure 3 shows that the rmsd of agonist,  $\alpha$  helix, and TM3 remains stable. Details can be found in the Supporting Information, Figure S1. The total energy of the system is equilibrated within 6 ns. In comparison, our molecular dynamics results of the  $\beta_2$ AR-Gs protein complex without a nanobody bound show sequential conformation changes, which will be discussed in detail in the following sections.

**3.2. Conformational Changes of Agonist without a Nanobody.** In order to study the interaction between the agonist-bound  $\beta_2$ AR and Gs protein and the impact of the artificial nanobody, we perform 20 ns molecular dynamics simulation without a nanobody bound.

First, we can find in the Supporting Information, Figure S2, the total energy of the system without a nanobody is equilibrated within 8 ns. Moreover, we can find that the rmsd of agonist,  $\alpha$ -helix, and TMs also remains stable after 8 ns (more details can be found in the following discussions).

Figure 4a and 4c shows a schematic view of the interactions between BI-167107 and  $\beta_2$ AR in the crystal structure (PDB entry 3SN6), which are almost the same as those in the crystal structure (without Gs protein) of a nanobody-stabilized active state of  $\beta_2$ AR reported by Rasmussen.<sup>7</sup> The mutations of amino acids reported by other groups,<sup>2,3,5,7</sup> including Asp<sup>3,32</sup>, Ser<sup>5,42</sup>, Ser<sup>5,43</sup>, Ser<sup>5,46</sup>, Asn<sup>6,55</sup>, Tyr<sup>7,35</sup>, and Asn<sup>7,39</sup>, affect binding significantly. Asp<sup>3,32</sup> in TM3, Ser<sup>5,42</sup> and Ser<sup>5,46</sup> in TMS, Asn<sup>6,55</sup> in TM6, and Asn<sup>7,39</sup> in TM7 form polar interactions with the agonist. The hydrophobic residues Trp<sup>3,28</sup>, Val<sup>3,36</sup>, Phe<sup>5,32</sup>, Tyr<sup>5,38</sup>, Ala<sup>5,39</sup>, Ser<sup>5,43</sup>, Phe<sup>6,51</sup>, Phe<sup>6,52</sup>, Tyr<sup>7,35</sup>, and Ile<sup>7,36</sup> interact with a ligand similar to those in the crystal structure (without Gs protein) of a nanobody-stabilized active state of  $\beta_2$ AR reported by Rasmussen et al.

Figure 4b and 4d shows a schematic view of the interactions between BI-167107 and  $\beta_2$ AR after 20 ns equilibration MD simulations without a nanobody bound. Our results show that the hydrogen bond between Asp<sup>3,32</sup> and alkylamine and that between Asn<sup>7,39</sup> and  $\beta$ -OH/alkylamine reamin stable during MD simulations. Our MD results show that the alkylamine and phenyl ring of BI-167107 move toward TM3, while the alkylamine of the ligand tightly interacts with Asp<sup>3,32</sup> (see the Supporting Information, Figure S3, for detail). Moreover, our results show that the heterocycle of BI-167107 moves upward to get close to EL2 during the first 2 ns MD, moving toward TM6. The interactions between the heterocycle of BI-167107 and receptor change significantly. The hydrogen bond between  $\beta$ -OH and Ser<sup>5,46</sup> breaks and forms hydrogen bonds with Ser<sup>5,42</sup> and Ser<sup>5,43</sup> tightly (Supporting Information, Figure S3). The

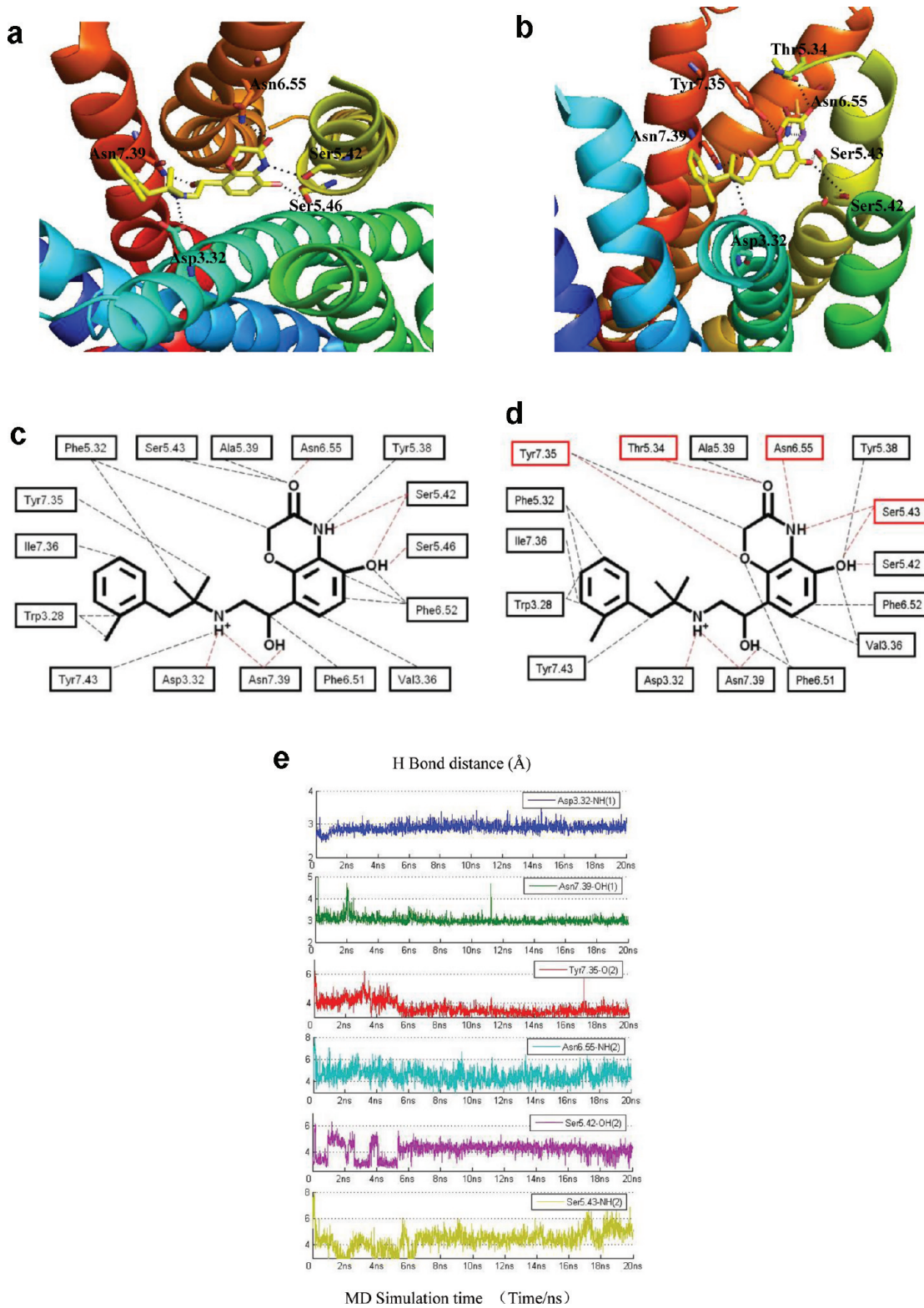


**Figure 4.** (a) Hydrogen bonds formed between BI-167107 and  $\beta_2\text{AR}$  with a nanobody bound in the crystal structure (PDB entry 3SN6). (b) Hydrogen bonds formed between BI-167107 and  $\beta_2\text{AR}$  without a nanobody bound after 20 ns MD equilibration. There are more hydrogen bonds formed after MD simulation. (c) Schematic view of the interactions between BI-167107 and  $\beta_2\text{AR}$  in the crystal structure (PDB entry 3SN6): hydrophobic contacts are shown as gray dashed lines, and hydrogen bonds are highlighted in red. (d) Schematic view of the interactions between BI-167107 and  $\beta_2\text{AR}$  without a nanobody bound after 20 ns MD: hydrophobic contacts are shown as gray dashed lines, and hydrogen bonds are highlighted in red. Residues formed new hydrogen bonds after 20 ns MD are highlighted in red. (e) Time evolution of hydrogen-bond distances between BI-167107 and  $\beta_2\text{AR}$  without a nanobody during 20 ns molecular dynamics.

carbonyl ( $=\text{O}$ ) of heterocycle forms a hydrogen bond with  $\text{Thr}^{5.34}$ , and the  $-\text{NH}$  of the heterocycle forms a hydrogen

bond with residue  $\text{Asn}^{6.55}$ , while another carbonyl ( $=\text{O}$ ) of heterocycle forms a polar interaction with  $\text{Tyr}^{7.35}$ . The

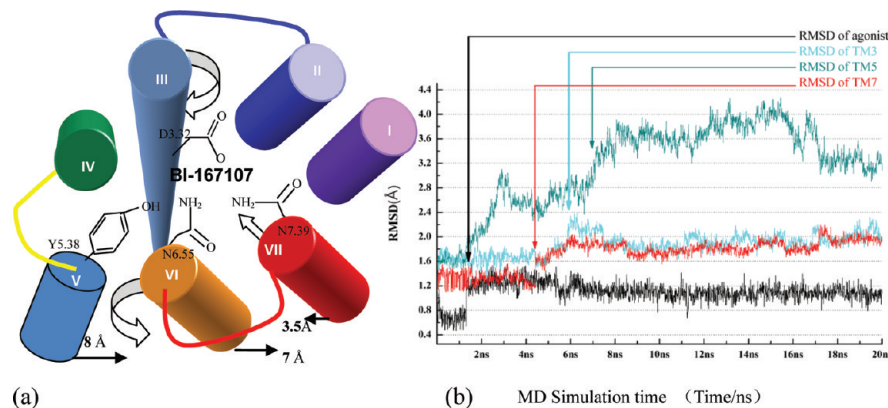


**Figure 5.** (a) Cartoon showing the conformational change of  $\beta_2$ AR during 20 ns MD simulations without a nanobody bound. Binding pocket of the  $\beta_2$ AR and agonist has conformational changes including Asp<sup>3.32</sup>, Tyr<sup>5.38</sup>, Asn<sup>6.55</sup>, and Asn<sup>7.39</sup>. TM3 makes a clockwise rotation due to a rotation and a movement of Asp<sup>3.32</sup>. Intracellular part of TM5 moves to TM6 for  $\sim 8 \text{ \AA}$ . TM6 makes a counter-clockwise rotation, and the intracellular part of it moves outward for  $\sim 7 \text{ \AA}$ , while TM7 moves inward and the intracellular part of TM7 moves for  $\sim 3.5 \text{ \AA}$ . (b) Time evolution of rmsd of the agonist and TMs. Agonist makes the conformational change around 1.5 ns. TM7 makes the conformational change around 4.5 ns. TM3 makes the conformational change around 6 ns. TM5 makes the conformational change around 7 ns.

hydrophobic interactions with Trp<sup>3.28</sup>, Val<sup>3.36</sup>, Phe<sup>5.32</sup>, Phe<sup>6.51</sup>, Tyr<sup>7.43</sup>, and Ile<sup>7.36</sup> make some changes (Figure 4d). With the conformational change of the ligand, we find that the percentages of formation of the hydrogen bond remain stable. During the first 6 ns simulation, there are 6 pairs of hydrogen bonds. After 14 ns simulation, we find 9 pairs of hydrogen bonds. These results indicate that the agonist BI-167107 has the flexibility to interact with the  $\beta_2$ AR with different H-bond partners, which facilitates its role in the activation of  $\beta_2$ AR (see the Supporting Information, Figure S3, for details, and the residues discussed in this section are in the extracellular region).

**3.3. Conformational Change of  $\beta_2$ AR without a Nanobody.** Figure 5 shows the conformational change of  $\beta_2$ AR during 20 ns MD simulations without a nanobody bound. The binding pocket of  $\beta_2$ AR has conformational changes including Asp<sup>3.32</sup>, Tyr<sup>5.38</sup>, Asn<sup>6.55</sup>, and Asn<sup>7.39</sup>. TM3 makes a clockwise rotation due to rotation and movement of Asp<sup>3.32</sup> (see the Supporting Information, Figure S4a, for details). The intracellular part of TM5 moves to TM6 for  $\sim 8 \text{ \AA}$ . TM6 makes a counter-clockwise rotation, and the intracellular part moves outward for  $\sim 7 \text{ \AA}$ , while TM7 moves inward, and the intracellular part of TM7 moves for  $\sim 3.5 \text{ \AA}$ .

Figure S4a (Supporting Information, Figure S4) shows that Trp<sup>6.48</sup>, a highly conserved residue in GPCRs, makes an upward movement and counter-clockwise rotation. The rotameric state of this residue is important for activation.<sup>7,44–46</sup> However, our results illustrate there is no change for a side chain rotamer of Trp<sup>6.48</sup>, which agrees with recent mutagenesis experiments on the serotonin SHT4 receptor and the crystal structures of A<sub>2A</sub>AR and  $\beta_2$ .<sup>7,44–46</sup> Similarly, Asn<sup>7.39</sup> moves inward (toward to TM3) and upward (toward to the extracellular) to form a tightly polar interaction with the alkylamine of BI-167107.

Figures S4b and S4c (Supporting Information, Figure S4) highlight the conformational changes of seven trans-membrane regions. Our results show that TM3, TM5, TM6, and TM7 make significant conformational changes, which is in agreement with previous studies.<sup>7,44–46</sup> TM3, TM5, and TM6 move outward, while TM7 moves inward. After 20 ns MD simulations, TM3, TM5, TM6, and TM7 fluctuate  $\sim 2.1$ ,  $\sim 3.3$ ,  $\sim 2.1$ , and  $\sim 2.0 \text{ \AA}$ , respectively.

We find TM1, TM2, and TM4 make movements too. Previous studies<sup>7</sup> show TM1, TM2, and TM4 do not make

significant movements for other GPCRs. For  $\beta_2$ AR, our results show that TM1 moves inward while TM2 and TM4 move outward. After 20 ns MD simulations, TM1, TM2, and TM4 fluctuate  $\sim 2.0$ ,  $\sim 1.7$ , and  $\sim 2.7 \text{ \AA}$ , respectively.

TM4 makes more significant movement than TM3, TM6, or TM7. Figure S4d, Supporting Information, shows that side chains of several residues in TM4 make conformational changes.

The sequence studies of  $\beta_2$ AR among humans revealed that two coding SNPs including Arg<sup>16</sup>Gly and Gln<sup>27</sup>Glu occur commonly,<sup>47</sup> both of which had been implicated in the response to agonists. A third nonsynonymous SNP, Thr<sup>164</sup>Ile, was less common but important.<sup>48–50</sup> Some studies<sup>32,51</sup> revealed that Thr<sup>164</sup>Ile SNP was rare, with the frequency of heterozygosity being 3–5% in all populations studied.<sup>52</sup> Meanwhile, a report<sup>53</sup> showed that all three SNPs<sup>54</sup> had functional effects,<sup>55</sup> and Thr<sup>164</sup>Ile SNP decreased Gs protein coupling and responded to  $\beta_2$  agonists. These results are consistent with our MD results, where Thr164 shows significant flexibility.

For TM5, TM6, and TM7 we find that the motif “KRQLQKIDKSEGR” of TM5, motif “CLKEHKALK” of TM6, and motif “NPxxY” of TM7 make significant conformational changes. The deviations of “KRQLQKIDKSEGR”, “CLKEHKALK”, and “NPxxY” are  $\sim 3.0$ ,  $\sim 2.7$ , and  $\sim 2.2 \text{ \AA}$ , respectively. The motif “CLKEHKALK” of TM6 moves outward significantly. The motif “KRQLQKIDKSEGR” of TM5 rotates and moves toward to TM6. These particular motifs are the intracellular part of the receptor and tightly interact with the Gs protein.

Our results show that the TM5 C-terminal and TM6 N-terminal make great conformational changes without a nanobody bound. For comparison, with a nanobody bound, TM5 C-terminal and TM6 N-terminal do not make significant conformational changes (rmsd 1.27 and 1.36  $\text{\AA}$ ). In either simulation (with or without a nanobody bound), we do not include the missing loop, which connects TM5 and TM6. The great conformational changes of TM5 C-terminal and TM6 N-terminal without a nanobody bound are not caused by the missed loop in our simulation.

Tyr<sup>7.53</sup>, which belongs to the highly conserved “NPxxY” motif, makes a conformational change ( $\sim 1.5 \text{ \AA}$ ), which has

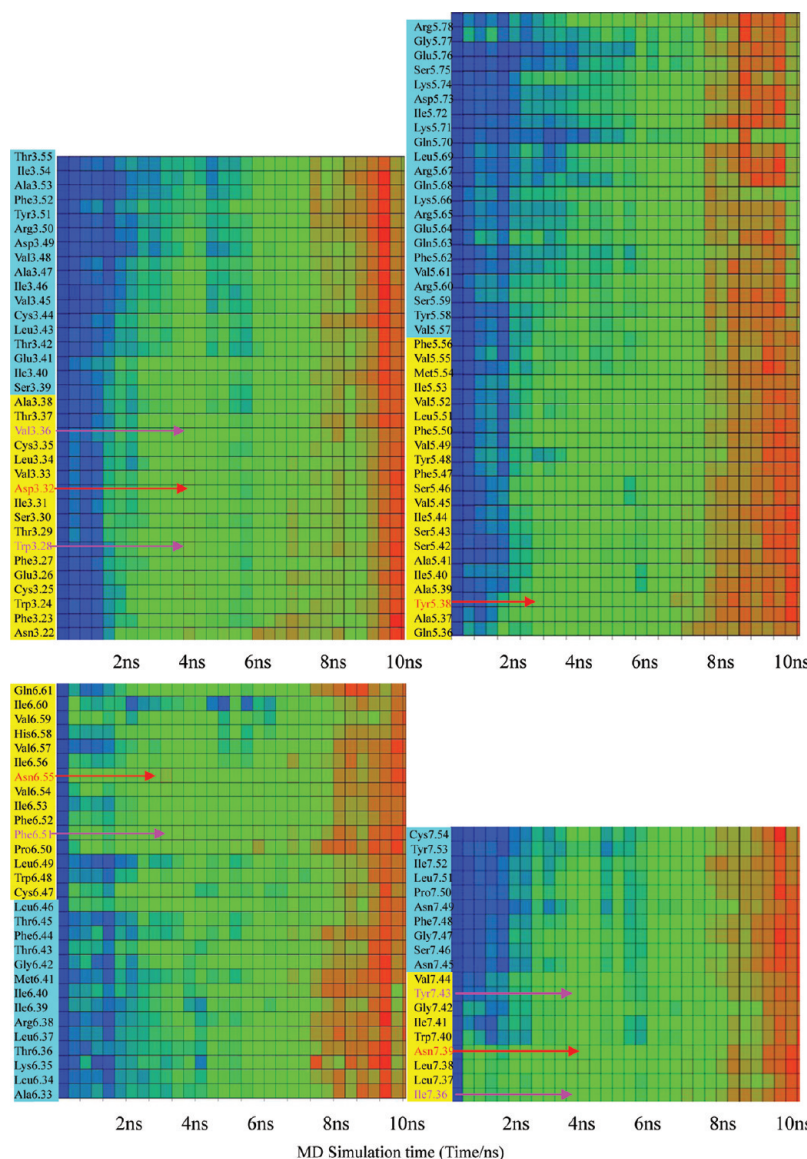


**Figure 6.** VmdICE plot of the rmsd of each residue of TM3, TM5, TM6, or TM7. Residues involved in the binding pocket including Asp<sup>3.32</sup>, Tyr<sup>5.38</sup>, Asn<sup>6.55</sup>, Asn<sup>7.39</sup>, Trp<sup>3.28</sup>, Val<sup>3.36</sup>, Phe<sup>6.51</sup>, Ile<sup>7.36</sup>, and Tyr<sup>7.43</sup> make conformational changes first, and the extracellular region of  $\beta_2$ AR makes the conformational change during the first 4–6 ns simulation. Intracellular region of  $\beta_2$ AR makes the conformational change at ~7 ns simulation. Time (ns) is on the x axis, residues are on the y axis, and colored data points refer to different rmsd values. Residues in yellow are in the extracellular region, while the residues in cyan are in the intracellular region. Red represents a strong fluctuation (it is the rmsd value, which is compared to the first frame of our simulation), and blue represents a weak fluctuation.

been implicated in the activation mechanism of GPCRs.<sup>7,44–46</sup> Our simulation results show that the backbone of the “NPXXY” motif makes strong conformational changes (~2.2 Å). These results are in agreement with recent studies.<sup>7,44–46</sup>

We use the vmdICE<sup>56</sup> program to show the rmsd for each residue that belongs to TM3, TM5, TM6, and TM7, and the results are shown in Figure 6.

The residues involved in the binding pocket in the extracellular parts (include Asp<sup>3.32</sup>, Tyr<sup>5.38</sup>, Asn<sup>6.55</sup>, and Asn<sup>7.39</sup>) make significant conformational changes during the first 4–6 ns. Meanwhile, several residues belonging to the binding pocket (include Trp<sup>3.28</sup>, Val<sup>3.36</sup>, Phe<sup>6.51</sup>, Ile<sup>7.36</sup>, and Tyr<sup>7.43</sup>) also make significant conformational changes during the first 4 ns. From Figure 6 we can see that the extracellular part of TM3 fluctuates significantly (red) around 6 ns, while the extracellular part of TM5 fluctuates dramatically around 7 ns.

The extracellular part of TM7 is around 6.6 ns. However, the intracellular part of  $\beta_2$ AR makes a conformational change after ~7 ns.

In conclusion, our results, particularly Figure 6, show that  $\beta_2$ AR makes a conformational change sequentially from the extracellular part to the intracellular region. (All residues discussed in this section are in the extracellular region.)

**3.4. Conformational Change of the Interface Between the  $\beta_2$ AR and Gs-Protein without a Nanobody.** The  $\alpha 5$ -helix of the Gs protein directly interacts with the intracellular parts of  $\beta_2$ AR, including the intracellular part of TM3, TM5, TM6, and TM7. Figure 7 shows that the conformational change of the  $\alpha 5$ -helix, which is correlated with the conformational change of TM3, TM5, TM6, and TM7 of  $\beta_2$ AR.

Figure S5, Supporting Information, shows the interface between the  $\beta_2$ AR and Gs protein in the crystal structure and

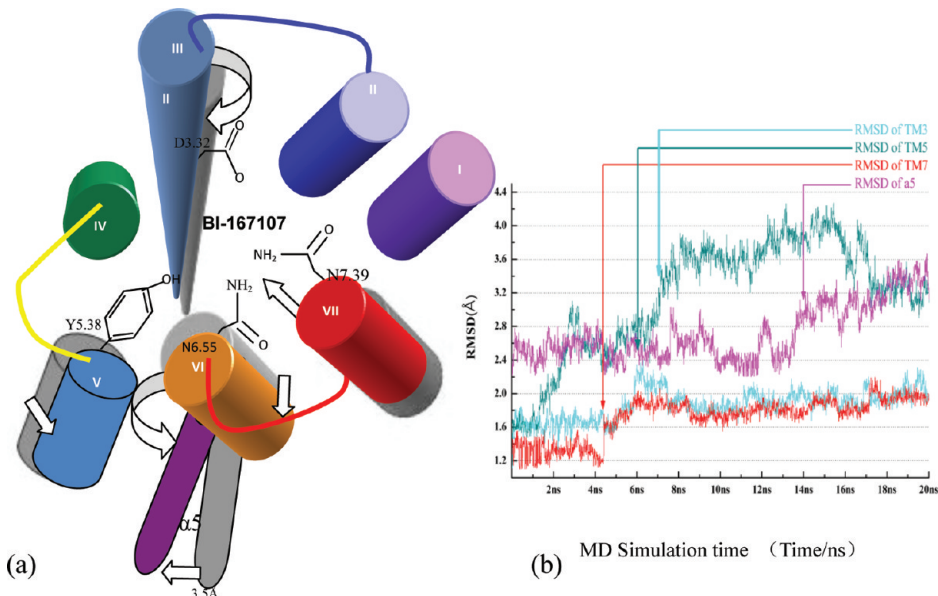


**Figure 7.** Cartoon showing the conformational change of the  $\alpha_5$ -helix of the Gs protein interacting with TM3, TM5, TM6, and TM7 without a nanobody bound. TMs highlighted in gray are the conformation from the crystal structure, and TMs highlighted in different colors are the conformation after 20 ns MD. Figure on right shows the time evolution of rmsd of TMs and  $\alpha_5$ -helix. TMs make conformation changes first, and then the  $\alpha_5$ -helix makes a conformational change at  $\sim$ 14 ns.

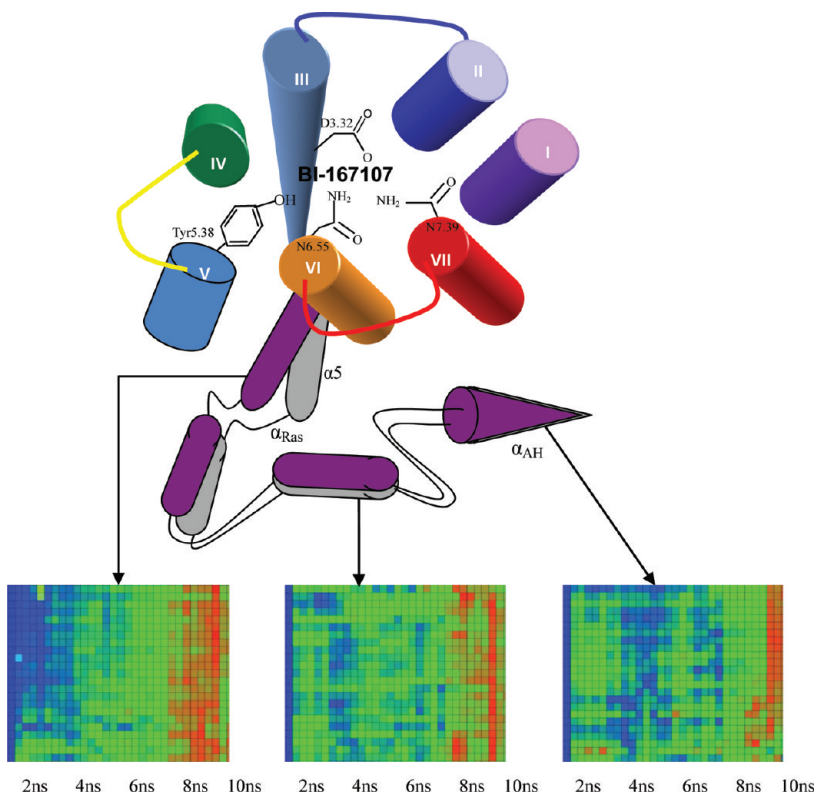


**Figure 8.** Cartoon showing conformational changes of different parts of the Gs protein.  $\alpha_5$ -helix makes a significant conformational change. In comparison,  $\alpha_{\text{Ras}}$  and  $\alpha_{\text{AH}}$  make less conformational change. Meanwhile, different parts of  $\alpha_{\text{Ras}}$  and  $\alpha_{\text{AH}}$  make conformational changes in a sequence according to their distances to  $\beta_2$ AR.

the interface structure after 20 ns MD simulations without a nanobody bound.

Our results (Supporting Information, Figure S5) show that Asp<sup>3.49</sup>, Ala<sup>3.53</sup>, and Thr<sup>3.55</sup> in TM3 of  $\beta_2$ AR tightly interact with residues Tyr<sup>391</sup>, His<sup>387</sup>, and Arg<sup>380</sup> of the  $\alpha_5$ -helix during our MD simulations. Arg<sup>380</sup> of the  $\alpha_5$ -helix has a significant

conformational change during MD simulations due to the interaction with Thr<sup>3.55</sup> of TM3. Glu<sup>390</sup> of the  $\alpha_5$ -helix makes a side chain conformational change and forms a hydrogen bond with Tyr<sup>3.60</sup> of IL2.

The interactions between Glu<sup>5.64</sup>, Arg<sup>5.67</sup>, and Gln<sup>5.68</sup> of TMS and Arg<sup>385</sup>, Glu<sup>384</sup>, and Asp<sup>381</sup> of the  $\alpha_5$ -helix remain stable

during MD simulations. Comparing Figures S5c and S5f, Supporting Information, we can see that the interaction between Arg<sup>755</sup> in TM7 and Glu<sup>392</sup> in the  $\alpha$ 5-helix remains stable, so does the interaction between Lys<sup>632</sup> in TM6 and Leu<sup>394</sup> in the  $\alpha$ 5-helix.

We find that the interaction between Asp<sup>349</sup> and Tyr<sup>360</sup> remains stable, and the IL2 helix is stabilized by this interaction. Tyr<sup>360</sup> has been shown to be a substrate for the insulin receptor tyrosine kinase:<sup>2,57</sup> phosphorylation of tyrosyl residues of  $\beta_2$ AR was obligatory for counter-regulation by insulin, suggesting the hypothesis that Gs-protein-linked receptors themselves may act as substrates for the insulin receptor and other growth factor receptors.

The residues involved in the hydrophobic interactions between the receptor and the Gs protein also make conformational changes. For example, Phe<sup>358</sup> in IL2 involved in the hydrophobic pocket (including several residues of the Gs protein: V217, I383, and F379) maintains a strong hydrophobic interaction with the Gs protein and makes a conformational change. This is consistent with the fact that mutant Phe<sup>358</sup>Ala has severely impaired coupling to Gs.<sup>2</sup>

Figure S6, Supporting Information, shows that the conformational change of  $\alpha$ 5-helix is due to the conformational changes of the interface between the  $\beta_2$ AR and Gs protein. The rmsd of the  $\alpha$ 5-helix is about 3.5 Å.

Our results show that the conformational change of  $\beta_2$ AR, especially in TM3, TM5, TM6, and TM7, induces a conformational change in the interface between the  $\beta_2$ AR and Gs protein, which leads to a conformational change of the Gs protein. (All residues discussed in this section are in the intracellular region of  $\beta_2$ AR.)

**3.5. Conformational Change of Gs Protein without a Nanobody.** Figure S7a, Supporting Information, shows that the conformational change of  $\alpha_{\text{Ras}}$  of the Gs protein. The rmsd after 20 ns MD of  $\alpha_{\text{Ras}}$  is ~3.1 Å. Figure S7b, Supporting Information, shows the conformational change of  $\alpha_{\text{AH}}$  of the Gs protein. The rmsd after 20 ns MD of  $\alpha_{\text{AH}}$  is ~2.7 Å.

We use the vmdICE<sup>56</sup> program to show the rmsd for each residue of different parts of  $\alpha_{\text{Ras}}$  (including the  $\alpha$ 5-helix) and  $\alpha_{\text{AH}}$ . Figure 8 shows that rmsd becomes small in a sequence of  $\alpha$ 5-helix,  $\alpha_{\text{Ras}}$ , and  $\alpha_{\text{AH}}$ . The rmsd becomes small because these three parts have different distances (from short to long) to  $\beta_2$ AR.

As shown in Figure 8, the  $\alpha$ 5-helix first makes the conformational change at ~7.5 ns, which corresponds to the conformational change of the intracellular part of  $\beta_2$ AR at ~7 ns. In comparison, the distal part of  $\alpha_{\text{Ras}}$  makes the conformational change at ~8.5 ns first, while  $\alpha_{\text{AH}}$  of the Gs protein first makes the conformational change after 9.5 ns. Different parts of  $\alpha_{\text{Ras}}$  and  $\alpha_{\text{AH}}$  make conformational changes in a sequence according to their distances to  $\beta_2$ AR.

**3.6. Sequential Conformational Change in Gs- $\beta_2$ AR Complex without a Nanobody.** Figure 9 shows sequential conformational changes of the Gs protein- $\beta_2$ AR complex during MD simulation: (1) an agonist-bound part of  $\beta_2$ AR; (2) the intracellular region of  $\beta_2$ AR; (3) the Gs protein (more detail can be found in Figure S8, Supporting Information). Different parts of the Gs protein make conformational changes sequentially according to their distances to  $\beta_2$ AR. Our results provide a structural basis for the study of the conformational change (conformational change of  $\beta_2$ AR sequentially from the extracellular region to the intracellular region) and the activation mechanism of  $\beta_2$ AR and other GPCRs.

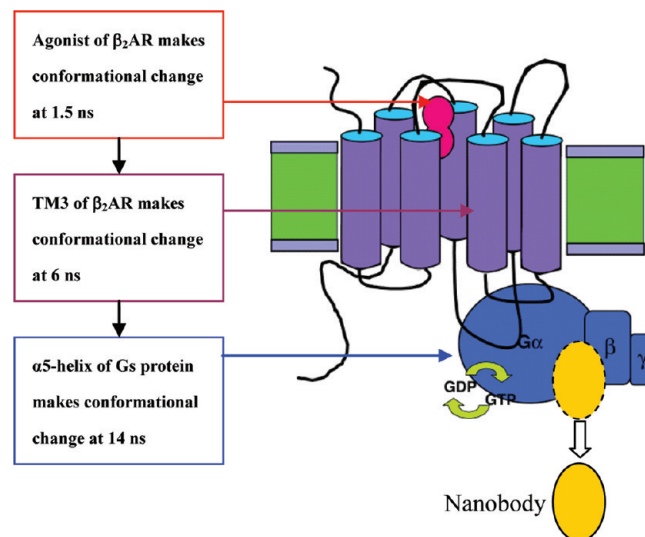


**Figure 9.** Without a nanobody bound, the  $\beta_2$ AR-Gs protein complex makes conformational changes in the following sequence: (1) agonist bound part of  $\beta_2$ AR; (2) intracellular region of  $\beta_2$ AR; (3) Gs protein. Different parts of the Gs protein make conformational changes sequentially according to their distances to  $\beta_2$ AR.

## 4. CONCLUSION

On the basis of the recently available high-resolution structure of the  $\beta_2$ AR-Gs protein complex, we perform MD simulations of the complex with ligand bound in explicit lipid and water. Without a nanobody stabilized,  $\beta_2$ AR makes conformational changes from the extracellular region to the intracellular region. The interactions between the  $\alpha$ 5-helix of the Gs protein and  $\beta_2$ AR make the  $\alpha$ 5-helix move significantly. Different parts of the Gs protein make conformational changes sequentially according to their distances to  $\beta_2$ AR. In comparison, with a nanobody bound, the  $\beta_2$ AR and the Gs protein remains stable in molecular dynamics simulation.

Our results show sequential conformational changes of the  $\beta_2$ AR-Gs protein complex: (1) an agonist-bound pocket of  $\beta_2$ AR; (2) the intracellular region of  $\beta_2$ AR; (3) the Gs protein. Our results provide a structural basis for the study of conformational change (conformational change of  $\beta_2$ AR sequentially from the extracellular region to the intracellular region) and the activation mechanism of  $\beta_2$ AR and other GPCRs.

## ■ ASSOCIATED CONTENT

### S Supporting Information

Figures S1-S8. The RMSD of TM5 and TM7 keep stable after 6 ns (Figure S1); the total energy of the system without a nanobody is equilibrated within 8 ns (Figure S2); conformational change of the agonist without a nanobody bound after 20 ns MD (Figure S3); the conformational change of residues involved in the binding pocket and the receptor (Figure S4); the conformational change of the interface between Gs protein and  $\beta_2$ AR (Figure S5); the conformational change of  $\alpha$ 5-helix of Gs protein (Figure S6); the conformational changes of  $\alpha_{\text{Ras}}$  and  $\alpha_{\text{AH}}$  of Gs (Figure S7); the sequential conformational changes of Gs protein- $\beta_2$ AR (Figure S8). This material is available free of charge via the Internet at <http://pubs.acs.org>.

## AUTHOR INFORMATION

### Corresponding Author

\*E-mail: yyli@suda.edu.cn.

### Notes

The authors declare no competing financial interest.

## ACKNOWLEDGMENTS

We acknowledge a grant from the National Basic Research Program of China (973 Program, Grant Nos. 2012CB932400 and 2010CB934500), the National Natural Science Foundation of China (Grant No. 21003091), the Natural Science Foundation of Jiangsu Province (Grant No. BK2010216), and a Project Funded by the Priority Academic Program Development of Jiangsu Higher Education Institutions (PAPD).

## REFERENCES

- (1) Hausch, F. Betablockers at work: The crystal structure of the beta(2)-adrenergic receptor. *Angew. Chem., Int. Ed.* **2008**, *47*, 3314–3316.
- (2) Rasmussen, S. G. F.; DeVree, B. T.; Zou, Y. Z.; Kruse, A. C.; Chung, K. Y.; Kobilka, T. S.; Thian, F. S.; Chae, P. S.; Pardon, E.; Calinski, D.; Mathiesen, J. M.; Shah, S. T. A.; Lyons, J. A.; Caffrey, M.; Gellman, S. H.; Steyaert, J.; Skiniotis, G.; Weis, W. I.; Sunahara, R. K.; Kobilka, B. K. Crystal structure of the beta(2) adrenergic receptor-Gs protein complex. *Nature* **2011**, *477*, 549–555.
- (3) Rasmussen, S. G. F.; Choi, H. J.; Rosenbaum, D. M.; Kobilka, T. S.; Thian, F. S.; Edwards, P. C.; Burghammer, M.; Ratnala, V. R. P.; Sanishvili, R.; Fischetti, R. F.; Schertler, G. F. X.; Weis, W. I.; Kobilka, B. K. Crystal structure of the human beta(2) adrenergic G-protein-coupled receptor. *Nature* **2007**, *450*, 383–387.
- (4) Nobles, K. N.; Xiao, K. H.; Ahn, S.; Shukla, A. K.; Lam, C. M.; Rajagopal, S.; Strachan, R. T.; Huang, T. Y.; Bressler, E. A.; Hara, M. R.; Shenoy, S. K.; Gygi, S. P.; Lefkowitz, R. J. Distinct Phosphorylation Sites on the beta(2)-Adrenergic Receptor Establish a Barcode That Encodes Differential Functions of beta-Arrestin. *Sci. Signal.* **2011**, *4*, ra51.
- (5) Cherezov, V.; Rosenbaum, D. M.; Hanson, M. A.; Rasmussen, S. G. F.; Thian, F. S.; Kobilka, T. S.; Choi, H. J.; Kuhn, P.; Weis, W. I.; Kobilka, B. K.; Stevens, R. C. High-resolution crystal structure of an engineered human beta(2)-adrenergic G protein-coupled receptor. *Science* **2007**, *318*, 1258–1265.
- (6) Reynolds, K. A.; Katritch, V.; Abagyan, R. Identifying conformational changes of the beta(2) adrenoceptor that enable accurate prediction of ligand/receptor interactions and screening for GPCR modulators. *J. Comput.-Aided. Mol. Des.* **2009**, *23*, 273–288.
- (7) Rasmussen, S. G. F.; Choi, H. J.; Fung, J. J.; Pardon, E.; Casarosa, P.; Chae, P. S.; DeVree, B. T.; Rosenbaum, D. M.; Thian, F. S.; Kobilka, T. S.; Schnapp, A.; Konetzki, I.; Sunahara, R. K.; Gellman, S. H.; Pautsch, A.; Steyaert, J.; Weis, W. I.; Kobilka, B. K. Structure of a nanobody-stabilized active state of the beta(2) adrenoceptor. *Nature* **2011**, *469*, 175–180.
- (8) Wojtowicz, A.; Fidzinski, P.; Heinemann, U.; Behr, J. Beta-adrenergic receptor activation induces long-lasting potentiation in burst-spiking but not regular-spiking cells at CA1-subiculum synapses. *Neuroscience* **2010**, *171*, 367–372.
- (9) Mitropoulos, D.; Kyroudi-Voulgari, A.; Stratigea, F.; Perea, D.; Boudoulas, H.; Karayannacos, P. Beta-adrenergic receptor blockade and prostate peptide growth factor expression in the rat. *Immunopharmacol. Immunotox.* **2010**, *32*, 105–109.
- (10) Queen, L.; Ferro, A. Beta-adrenergic receptors and nitric oxide generation in the cardiovascular system. *Cell. Mol. Life Sci.* **2006**, *63*, 1070–1083.
- (11) Hanania, N. A.; Dickey, B. F.; Bond, R. A. Clinical implications of the intrinsic efficacy of beta-adrenoceptor drugs in asthma: full, partial and inverse agonism. *Curr. Opin. Pulm. Med.* **2009**, *16*, 1–5.
- (12) Metra, M.; Covolo, L.; Pezzali, N.; Zaca, V.; Bugatti, S.; Lombardi, C.; Bettari, L.; Romeo, A.; Gelatti, U.; Giubbini, R. Role of beta-adrenergic receptor gene polymorphisms in the long-term effects of beta-blockade with carvedilol in patients with chronic heart failure. *Cardiovasc. Drug Ther.* **2010**, *24*, 49–60.
- (13) Mangmool, S.; Shukla, A. K.; Rockman, H. A. beta-Arrestin-dependent activation of Ca(2+)/calmodulin kinase II after beta(1)-adrenergic receptor stimulation. *J. Cell. Biol.* **2010**, *189*, 573–587.
- (14) Nussinovitch, U.; Shoenfeld, Y. The clinical significance of anti-beta-1 adrenergic receptor autoantibodies in cardiac disease. *Clin. Rev. Allergy Immunol.* **2010**, *1*–9.
- (15) Nakajima, Y.; Imanishi, M.; Itou, S.; Hamashima, H.; Tomishima, Y.; Washizuka, K.; Sakurai, M.; Matsui, S.; Imamura, E.; Ueshima, K. Discovery of novel series of benzoic acid derivatives containing biphenyl ether moiety as potent and selective human [beta] 3-adrenergic receptor agonists: Part IV. *Bioorg. Med. Chem. Lett.* **2008**, *18*, 5037–5040.
- (16) Leon, L. A.; Hoffman, B. E.; Gardner, S. D.; Laping, N. J.; Evans, C.; Lashinger, E. S. R.; Su, X. Effects of the beta 3-adrenergic receptor agonist disodium 5-[(2R)-2-[[2(R)-2-(3-chlorophenyl)-2-hydroxyethyl] amino] propyl]-1, 3-benzodioxole-2, 2-dicarboxylate (CL-316243) on bladder micturition reflex in spontaneously hypertensive rats. *J. Pharmacol. Exp. Ther.* **2008**, *326*, 178–185.
- (17) De Luis, D.; Aller, R.; Izaola, O.; Gonzalez Sagrado, M.; Conde, R. Relation of Trp64Arg polymorphism of beta 3-adrenergic receptor gene to adipocytokines and fat distribution in obese patients. *Ann. Nutr. Metab.* **2008**, *52*, 267–271.
- (18) Aranguiz-Urroz, P.; Canales, J.; Copaja, M.; Troncoso, R.; Vicencio, J. M.; Carrillo, C.; Lara, H.; Lavandero, S.; Diaz-Araya, G. Beta2-adrenergic receptor regulates cardiac fibroblast autophagy and collagen degradation. *BBA-Mol. Basis Dis.* **2011**, *1812*, 23–31.
- (19) Li, Y.; Hou, T.; Goddard, I. Computational modeling of structure-function of G protein-coupled receptors with applications for drug design. *Curr. Med. Chem.* **2010**, *17*, 1167–1180.
- (20) Li, Y.; Hou, T. Computational Simulation of Drug Delivery at Molecular Level. *Curr. Med. Chem.* **2010**, *17*, 4482–4491.
- (21) Goddard, W. A. III; Kim, S. K.; Li, Y.; Trzaskowski, B.; Griffith, A. R.; Abrol, R. Predicted 3D structures for adenosine receptors bound to ligands: Comparison to the crystal structure. *J. Struct. Biol.* **2010**, *170*, 10–20.
- (22) Kim, S. K.; Li, Y.; Abrol, R.; Heo, J.; Goddard, W. A. III. Predicted Structures and Dynamics for Agonists and Antagonists Bound to Serotonin 5-HT2B and 5-HT2C Receptors. *J. Chem. Inf. Model.* **2011**, *51*, 420–433.
- (23) Li, Y.; Zhu, F.; Vaidehi, N.; Goddard, W. A. III; Sheinerman, F.; Reiling, S.; Morize, I.; Mu, L.; Harris, K.; Ardati, A. Prediction of the 3D structure and dynamics of human DP G-protein coupled receptor bound to an agonist and an antagonist. *J. Am. Chem. Soc.* **2007**, *129*, 10720–10731.
- (24) Kim, S. K.; Li, Y.; Park, C.; Abrol, R.; Goddard, W. A. III. Prediction of the Three-Dimensional Structure for the Rat Urotensin II Receptor, and Comparison of the Antagonist Binding Sites and Binding Selectivity between Human and Rat Receptors from Atomistic Simulations. *ChemMedChem* **2010**, *5*, 1594–1608.
- (25) Takeda, S.; Kadokawa, S.; Haga, T.; Takaesu, H.; Mitaku, S. Identification of G protein-coupled receptor genes from the human genome sequence. *Febs. Lett.* **2002**, *520*, 97–101.
- (26) Giembycz, M.; Newton, R. Beyond the dogma: novel beta2-adrenoceptor signalling in the airways. *Eur. Respir. J.* **2006**, *27*, 1286–1306.
- (27) Johnson, M. Molecular mechanisms of beta(2)-adrenergic receptor function, response, and regulation. *J. Allergy Clin. Immunol.* **2006**, *117*, 18–24.
- (28) Bateman, E. D.; Boushey, H. A.; Bousquet, J.; Busse, W. W.; Clark, T. J. H.; Pauwels, R. A.; Pedersen, S. E. Can guideline-defined asthma control be achieved?: The Gaining Optimal Asthma Control study. *Am. J. Respir. Crit. Care* **2004**, *170*, 836–844.
- (29) Gibson, P.; Powell, H.; Ducharme, F.; . Long-acting beta2-agonists as an inhaled corticosteroid-sparing agent for chronic asthma in adults and children. *Cochrane. DB. Syst. Rev.* **2005**, *4*.

- (30) O'Byrne, P. M.; Barnes, P. J.; Rodriguez-Roisin, R.; Runnerstrom, E.; Sandstrom, T.; Svensson, K.; Tattersfield, A. Low dose inhaled budesonide and formoterol in mild persistent asthma. The OPTIMA randomized trial. *Am. J. Respir. Crit. Care* **2001**, *164*, 1392–1397.
- (31) Chung, L.; Waterer, G.; Thompson, P. Pharmacogenetics of beta2 adrenergic receptor gene polymorphisms, long-acting beta-agonists and asthma. *Clin. Exp. Allergy* **2011**, *41*, 312–326.
- (32) Mansur, A.; Fontes, R.; Canzi, R.; Nishimura, R.; Alencar, A.; De Lima, A.; Krieger, J.; Pereira, A. Beta-2 adrenergic receptor gene polymorphisms Gln27Glu, Arg16Gly in patients with heart failure. *BMC Cardiovasc. Disorders* **2009**, *9*, 50.
- (33) Tian, X.; Zhang, L.; Xu, W.; Liu, J.; Liang, J. Effects of cAMP and-Adrenergic Receptor Antagonists on the Function of Peripheral T Helper Lymphocytes in Patients with Heart Failure. *Neuroimmunomodulation* **2011**, *18*, 73–78.
- (34) Shi, Q.; Hou, Y.; Yang, Y.; Bai, G. Protective Effects of Glycyrrhizin against beta-Adrenergic Receptor Agonist-Induced Receptor Internalization and Cell Apoptosis. *Biol. Pharm. Bull.* **2011**, *34*, 609–617.
- (35) Scheerer, P.; Park, J. H.; Hildebrand, P. W.; Kim, Y. J.; Krauss, N.; Choe, H. W.; Hofmann, K. P.; Ernst, O. P. Crystal structure of opsin in its G-protein-interacting conformation. *Nature* **2008**, *455*, 497–502.
- (36) Pedretti, A.; Villa, L.; Mazzolari, A.; Vistoli, G. VEGA—an open platform to develop chemo-bio-informatics applications, using plug-in architecture and script programming. *J. Comput.-Aided. Mol. Des.* **2004**, *18*, 167–173.
- (37) Hsin, J.; Arkhipov, A.; Yin, Y.; Stone, J. E.; Schulten, K. Using VMD: an introductory tutorial. *Curr. Protoc. Bioinformatics* **2008**.
- (38) Jorgensen, W. L.; Chandrasekhar, J.; Madura, J. D.; Impey, R. W.; Klein, M. L. Comparison of simple potential functions for simulating liquid water. *J. Chem. Phys.* **1983**, *79*, 926.
- (39) Kalé, L.; Skeel, R.; Bhandarkar, M.; Brunner, R.; Gursoy, A.; Krawetz, N.; Phillips, J.; Shinozaki, A.; Varadarajan, K.; Schulten, K. NAMD2: Greater Scalability for Parallel Molecular Dynamics\*. *J. Comput. Phys.* **1999**, *151*, 283–312.
- (40) MacKerell, A. D.; Bashford, D.; Bellott, M.; Dunbrack, R. L.; Evanseck, J. D.; Field, M. J.; Fischer, S.; Gao, J.; Guo, H.; Ha, S.; Joseph-McCarthy, D.; Kuchnir, L.; Kuczera, K.; Lau, F. T. K.; Mattos, C.; Michnick, S.; Ngo, T.; Nguyen, D. T.; Prothom, B.; Reiher, W. E.; Roux, B.; Schlenkrich, M.; Smith, J. C.; Stote, R.; Straub, J.; Watanabe, M.; Wiorkiewicz-Kuczera, J.; Yin, D.; Karplus, M. All-atom empirical potential for molecular modeling and dynamics studies of proteins. *J. Phys. Chem. B* **1998**, *102*, 3586–3616.
- (41) Brooks, B. R.; Brucoleri, R. E.; Olafson, B. D. CHARMM: A program for macromolecular energy, minimization, and dynamics calculations. *J. Comput. Chem.* **1983**, *4*, 187–217.
- (42) Feller, S. E.; MacKerell, A. D. An improved empirical potential energy function for molecular simulations of phospholipids. *J. Phys. Chem. B* **2000**, *104*, 7510–7515.
- (43) Essmann, U.; Perera, L.; Berkowitz, M. L.; Darden, T.; Lee, H.; Pedersen, L. G. A smooth particle mesh Ewald method. *J. Chem. Phys.* **1995**, *103*, 8577–8593.
- (44) Choe, H. W.; Kim, Y. J.; Park, J. H.; Morizumi, T.; Pai, E. F.; Krauss, N.; Hofmann, K. P.; Scheerer, P.; Ernst, O. P. Crystal structure of metarhodopsin II. *Nature* **2011**, *471*, 651–655.
- (45) Isberg, V.; Balle, T.; Sander, T.; Jørgensen, F. S.; Gloriam, D. E. G Protein- and Agonist-Bound Serotonin 5-HT(2A) Receptor Model Activated by Steered Molecular Dynamics Simulations. *J. Chem. Inf. Model.* **2011**, *51*, 315–325.
- (46) Xu, F.; Wu, H. X.; Katritch, V.; Han, G. W.; Jacobson, K. A.; Gao, Z. G.; Cherezov, V.; Stevens, R. C. Structure of an Agonist-Bound Human A(2A) Adenosine Receptor. *Science* **2011**, *332*, 322–327.
- (47) Insel, P. Beta 2-Adrenergic Receptor Polymorphisms and Signaling: Do Variants Influence the "Memory" of Receptor Activation? *Sci. Signal.* **2011**, *4*, pe37.
- (48) Panebra, A.; Wang, W. C.; Malone, M. M.; Pitter, D. R. G.; Weiss, S. T.; Hawkins, G. A.; Liggett, S. B. Common ADRB2 haplotypes derived from 26 polymorphic sites direct beta2-adrenergic receptor expression and regulation phenotypes. *Plos One* **2010**, *5*, e11819.
- (49) Ortega, V. E.; Hawkins, G. A.; Peters, S. P.; Bleecker, E. R. Pharmacogenetics of the [beta] 2-Adrenergic Receptor Gene. *Immunol. Allergy Clin.* **2007**, *27*, 665–684.
- (50) Hawkins, G. A.; Tantisira, K.; Meyers, D. A.; Ampleford, E. J.; Moore, W. C.; Klanderman, B.; Liggett, S. B.; Peters, S. P.; Weiss, S. T.; Bleecker, E. R. Sequence, haplotype, and association analysis of ADRbeta2 in a multiethnic asthma case-control study. *Am. J. Respir. Crit. Care* **2006**, *174*, 1101–1109.
- (51) Weir, T. D.; Mallek, N.; Sandford, A. J.; Bai, T. R.; Awadh, N.; Fitzgerald, J.; Cockcroft, D.; James, A.; Liggett, S. B.; Pare, P. D. beta 2-Adrenergic receptor haplotypes in mild, moderate and fatal/near fatal asthma. *Am. J. Respir. Crit. Care* **1998**, *158*, 787–791.
- (52) Small, K. M.; McGraw, D. W.; Liggett, S. B. Pharmacology and physiology of human adrenergic receptor polymorphisms. *Annu. Rev. Pharmacol.* **2003**, *43*, 381–411.
- (53) Shukla, A. K.; Violin, J. D.; Whalen, E. J.; Gesty-Palmer, D.; Shenoy, S. K.; Lefkowitz, R. J. Distinct conformational changes in beta-arrestin report biased agonism at seven-transmembrane receptors. *Proc. Natl. Acad. Sci. USA* **2008**, *105*, 9988–9993.
- (54) Wechsler, M. E.; Lehman, E.; Lazarus, S. C.; Lemanske, R. F.; Boushey, Jr; H. A.; Deykin, A.; Fahy, J. V.; Sorkness, C. A.; Chinchilli, V. M.; Craig, T. J. beta-Adrenergic receptor polymorphisms and response to salmeterol. *Am. J. Respir. Crit. Care* **2006**, *173*, 519–526.
- (55) Liggett, S. B. Phosphorylation Barcoding as a Mechanism of Directing GPCR Signaling. *Sci. Signal.* **2011**, *4*, pe36.
- (56) Knapp, B.; Lederer, N.; Omasits, U.; Schreiner, W. vmdICE: A Plug-In for Rapid Evaluation of Molecular Dynamics Simulations using VMD. *J. Comput. Chem.* **2010**, *31*, 2868–2873.
- (57) Baltensperger, K.; Karoor, V.; Paul, H.; Ruoho, A.; Czech, M. P.; Malbon, C. C. The-adrenergic receptor is a substrate for the insulin receptor tyrosine kinase. *J. Biol. Chem.* **1996**, *271*, 1061–1064.